NASA TECHNICAL NOTE

NASA TN D-7766

NASA TN D-7766

(NASA-TN-D-7766) A METHOD FOR DETERMINING LOCAL ELASTOPLASTIC STRESS AND STRAIN IN METALLURGICALLY BONDED NOTCHED LAMINATES SUBJECTED TO A LOADING CYCLE (NASA) 23 p HC $3.00 CSCL 20K

N74-35307

Unclas

H1/32 52017

A METHOD FOR DETERMINING LOCAL ELASTOPLASTIC STRESS AND STRAIN IN METALLURGICALLY BONDED NOTCHED LAMINATES SUBJECTED TO A LOADING CYCLE

by J. A. Sova and John H. Crews, Jr.

Langley Research Center
Hampton, Va. 23665

NATIONAL AERONAUTICS AND SPACE ADMINISTRATION • WASHINGTON, D. C. • OCTOBER 1974

A METHOD FOR DETERMINING LOCAL ELASTOPLASTIC STRESS AND STRAIN IN METALLURGICALLY BONDED NOTCHED LAMINATES SUBJECTED TO A LOADING CYCLE

By J. A. Sova* and John H. Crews, Jr.
Langley Research Center

SUMMARY

A semianalytical method was developed for determining elastoplastic cyclic stresses and strains at notch roots in metallurgically bonded metal laminates. The method is based on the Neuber equation, which was used with an "effective" stress-strain curve for the laminate. It was applied to laminates containing a circular hole which were subjected to one cycle of reversed loading. The laminates consisted of two elasto-perfectly-plastic materials with different yield strengths and with either equal or different Young's moduli. A laminate of high-strength titanium alloy with alternate layers of commercially pure titanium was also analyzed.

The accuracy of the method was evaluated by comparing the stresses and strains with those calculated from a finite-element analysis. The results estimated by the simple method based on the Neuber equation agreed closely with the results computed from the more elaborate finite-element analysis.

INTRODUCTION

Metallurgically bonded laminates of different metals provide a combination of properties not offered by a single metal. For example, high-strength aluminum alloys are sometimes clad to improve corrosion resistance. Also, advanced laminated materials, such as strong titanium alloys interleaved with weaker materials, can combine high strength with high toughness (refs. 1 and 2).

Fatigue processes in laminates are not adequately understood, however. Cladding frequently reduces the fatigue strength of a strong aluminum alloy by as much as 50 percent (refs. 3, 4, and 5). Although some qualitative explanations have been offered in reference 3, the detrimental effect of the cladding is not understood quantitatively. Also, fatigue in laminates must be predictable before the new titanium laminates can be efficiently used in structures.

---

*NRC-NASA Resident Research Associate.

Because fatigue cracks normally start at stress concentrations, the local cyclic stress and strain must be analyzed accurately to estimate fatigue damage. The objective of this investigation was to develop a simple method to determine local stresses and strains in the individual layers of metallurgically bonded metal laminates. The case studied was a laminated sheet containing a circular hole and subjected to one cycle of reversed uniaxial load. The method is based on an equation proposed by Neuber (ref. 6) and an "effective" stress-strain curve. Two of the laminates studied were composed of two elasto-perfectly-plastic layers with different yield strengths and with either equal or different Young's moduli; a third, two-layer laminate, which simulated several alternate layers of high-strength titanium alloy and commercially pure titanium, was also studied. The local stresses and strains determined by the present method were compared with values independently computed by a more elaborate finite-element analysis.

SYMBOLS

A_t	total net-section area, m^2
E	Young's modulus, N/m^2
$\bar{E}$	effective Young's modulus, N/m^2
e	nominal net-section strain
Δe_i	excursion of nominal net-section strain corresponding to $\Delta\bar{S}_i$
K_T	theoretical elastic stress-concentration factor
K_ϵ	strain-concentration factor
K_σ	stress-concentration factor
P	load, N
r	radius of hole, m
S	nominal net-section stress, N/m^2
$\bar{S}$	effective nominal net-section stress, N/m^2

$\Delta\bar{S}_i$ excursion of effective nominal net-section stress for ith load excursion, N/m^2

t thickness, m

t_t total thickness, m

w width, m

ϵ local strain

$\Delta\epsilon_i$ excursion of local strain corresponding to $\Delta\bar{S}_i$

σ local stress, N/m^2

$\bar{\sigma}$ effective local stress, N/m^2

$\Delta\bar{\sigma}_i$ excursion of effective local stress corresponding to $\Delta\bar{S}_i$, N/m^2

Subscripts:

A layer A

B layer B

PROCEDURES

Figure 1 shows the configuration analyzed in this investigation: a uniaxially loaded laminate composed of two metallurgically bonded materials, A and B, and containing a circular hole. The strains at the interface of the metallurgically bonded layers are equal. To simplify the analysis, the strains were also assumed to be uniform throughout the laminate thickness. A value of 10 for the ratio $(w/2)/r$ was chosen because, for this value, the edges of the sheet do not significantly influence the stress distribution at the hole. The fatigue-critical points are on the X-axis at the edge of the hole. At these points, the stresses and strains, called "local" stresses and strains, were determined by the method based on the Neuber equation and by the finite-element procedure.

Method Based on the Neuber Equation

This section first reviews the procedure for estimating local stresses and strains in monotonically loaded single sheets, then extends the method to monotonically loaded laminates, and finally, describes a procedure applicable to cyclically loaded laminates.

Monotonically loaded single sheets.- For a monotonically loaded sheet, the Neuber equation relates the elastic stress-concentration factor K_T to the stress- and strain-concentration factors K_σ and K_ϵ. The equation, in the notation of the present paper, is

$$K_T^2 = K_\sigma K_\epsilon$$

which can be rewritten in terms of local stress and strain σ and ϵ and nominal net-section stress and strain S and e to give

$$\sigma\epsilon = K_T^2 Se \tag{1}$$

This form of the Neuber equation is valid even when the nominal net-section stress S extends into the plastic range. To use equation (1), the nominal strain e is obtained from the uniaxial stress-strain curve so that e corresponds to the stress S. For elastic nominal net-section loading, $e = S/E$ and the Neuber equation becomes

$$\sigma\epsilon = \frac{(K_T S)^2}{E} \tag{2}$$

The procedure to determine local stress and strain in a single sheet (ref. 7) is explained with the aid of figure 2(a). In thin sheets containing a circular hole, a state of nearly uniaxial stress exists at two fatigue-critical points at the edges of the holes. Therefore, the stress-strain behavior at the hole can be represented by the uniaxial stress-strain curve for the material, for example, curve 01 in figure 2(a). For a net-section stress S in a notched sheet, the intersection (point 1) of the stress-strain curve with the Neuber curve provides values of local stress and strain σ_1 and ϵ_1 which satisfy the Neuber equation and are also consistent with the uniaxial stress-strain behavior of the material.

Monotonically loaded laminates.- An approach like that for single sheets was used to determine local stresses and strains in laminates, but the Neuber equation was used with an "effective" stress-strain curve for the laminate. The effective stress-strain curve is that which would be obtained experimentally from a tensile test of an unnotched laminate. The effective stresses corresponding to measured strains could be derived by

dividing the applied load P by the total area of the laminate A_t. The uniaxial effective curve can be used to represent the effective stress-strain behavior at a notch. Alternatively, the same effective stress-strain curve could be constructed from the uniaxial stress-strain curves for the individual layers of a laminate. This graphic method was used in the present study. In figure 2(b), the dash-dot curve is the uniaxial effective stress-strain curve for the metallurgically bonded laminate composed of layers A and B. The effective stress $\bar{\sigma}$ corresponding to a given strain ϵ is

$$\bar{\sigma} = \frac{\sigma_A t_A + \sigma_B t_B}{t_t} \tag{3}$$

where t_A and t_B are the thicknesses of layers A and B, and t_t is the total thickness of the laminate.

The Neuber curve for the notched laminate is also shown in figure 2(b). To construct the Neuber curve, equations (1) and (2) were rewritten in terms of effective values $\bar{\sigma}$, $\bar{S}$, and $\bar{E}$. For elastic nominal loading of a laminate $\left(e = \bar{S}/\bar{E}\right)$, equation (2) becomes

$$\bar{\sigma}\epsilon = \frac{\left(K_T \bar{S}\right)^2}{\bar{E}} \tag{4}$$

where $\bar{\sigma}$ is the effective local stress, ϵ is the local strain, $\bar{S}$ is the effective net-section stress $\left(\bar{S} = P/A_t\right)$, and $\bar{E}$ is the effective Young's modulus for the laminate. The modulus of the effective stress-strain curve $\bar{E}$ can be derived analytically as

$$\bar{E} = \frac{E_A t_A + E_B t_B}{t_t} \tag{5}$$

For net-section yielding in either of the layers, equation (1) can be rewritten as

$$\bar{\sigma}\epsilon = K_T^2 \bar{S} e \tag{6}$$

where the nominal strain e corresponds to stress $\bar{S}$ on the effective stress-strain curve.

The intersection of the effective stress-strain curve with the Neuber curve (point 1 in fig. 2(b)) determines the local strain ϵ_1. The corresponding local stresses in materials A and B can be read from the individual stress-strain curves at the strain ϵ_1.

Cyclically loaded laminates.- For cyclically loaded laminates, the Neuber equation was rewritten in terms of excursions of local stress and strain in a form similar to that in reference 8 for single sheets. Equations (4) and (6) are used in the following forms:

For elastic excursions of $\bar{S}_i$,

$$\Delta\bar{\sigma}_i \Delta\epsilon_i = \frac{(K_T \Delta\bar{S}_i)^2}{\bar{E}} \tag{7}$$

and, for plastic excursions of $\bar{S}_i$,

$$\Delta\bar{\sigma}_i \Delta\epsilon_i = K_T{}^2 \Delta\bar{S}_i \Delta e_i \tag{8}$$

The values of $\Delta\bar{\sigma}_i$ and $\Delta\epsilon_i$ are the excursions of effective local stress and local strain corresponding to the ith excursion of effective nominal stress $\Delta\bar{S}_i$.

Figure 3 illustrates how these equations are used to analyze the effects of cyclic loads. The typical cycle of effective nominal stress in figure 3(a) has been segmented into excursions of effective nominal stress $\Delta\bar{S}_1$ and $\Delta\bar{S}_2$. For the first excursion $\Delta\bar{S}_1$, the Neuber equation (7) or (8) is evaluated and plotted, together with the effective stress-strain curve, in the first quadrant of the sketch in figure 3(b). The intersection of the curves (point 1) determines $\Delta\epsilon_1$. The corresponding local stresses in materials A and B are found on the individual stress-strain curves at the strain $\Delta\epsilon_1$. For the second excursion of nominal effective stress $\Delta\bar{S}_2$, point 1 is taken as the initial state. Equation (7) or (8) is evaluated for $\Delta\bar{S}_2$ and plotted relative to point 1. The effective stress-strain curve is constructed from the appropriate stress-strain curves for unloading and subsequent compressive loading of materials A and B. The intersection point 2 establishes $\Delta\epsilon_2$ for which the corresponding local stresses in materials A and B are found on the individual stress-strain curves.

The residual local stresses and strains are found by a procedure also illustrated in figure 3. To obtain the half-cycle residual strain and stresses, equation (7) or (8) is evaluated for the unloading excursion $\Delta\bar{S}_1$ and plotted relative to point 1. The intersection of the Neuber and effective stress-strain curves, point R_1 in figure 3(b), establishes the residual strain, and the corresponding residual stresses are found on the stress-strain curves for the materials A and B. The full-cycle residual strain and stresses at point R_2 are found in a similar manner to complete the first cycle of local behavior.

The Neuber equation was used in a cycle-by-cycle manner to estimate local stresses and strains in single sheets in references 7 and 8. Similarly, the Neuber equation could be repeatedly applied to estimate local stresses and strains in laminates for succeeding cycles.

Finite-Element Analysis

The accuracy of the method based on the Neuber equation was estimated by comparing the results with similar results from a finite-element analysis. The laminate shown in figure 1 was analyzed by the finite-element program described in reference 9. The ability of the program to determine accurately the elastoplastic cyclic stresses and strains in single sheets subjected to uniaxial load has been verified in reference 10.

The finite-element model is shown in figure 4. Because of symmetry, only one quadrant of the laminate was modeled. Element nodes along the X- and Y-axes were constrained against y- and x-displacements, respectively. The two layers of the finite-element model were created by first specifying triangular elements in terms of nodes at their vertices, in the conventional manner, and by then specifying "overlaid" elements by the same sets of nodes. The two layers were assigned properties to represent selected materials discussed in the next section. Small elements with linearly varying strain were used for regions near the hole, where strain gradients are high; larger elements with uniform strain were used for the remainder of the model.

For this finite-element model, an elastic stress-concentration factor of 2.64 was determined from reference 11. Although this value is slightly lower than the theoretical value of 2.72 in reference 12, 2.64 was used in the Neuber equations herein to eliminate errors due to finite-element approximations when comparing results obtained from the Neuber and finite-element methods.

METHOD APPLICATION AND DISCUSSION

Three laminates of materials with different mechanical properties were selected as test cases. These laminates were analyzed by both the method based on the Neuber equation and the finite-element procedure.

Selection of Laminates

The laminates analyzed in this study are shown in figure 5. Elasto-perfectly-plastic materials (F, G, and H) of different yield strengths are represented by the stress-strain curves in figure 5(a). Two laminates composed of layers of equal thickness were analyzed: a laminate composed of materials F and G having equal Young's moduli, and a laminate composed of materials F and H having different moduli.

A third laminate, shown in figure 5(b), was also analyzed; it is composed of five layers of annealed Ti-6Al-4V alloy with interface layers of annealed, commercially pure titanium. The thicknesses (from ref. 1) were 1.02 mm for the titanium alloy and 0.25 mm for the pure titanium. The stress-strain curves for these materials, obtained from references 13 and 14, are shown in figure 5(b).

Local Stresses and Strains in Laminates

The laminate composed of materials F and G (equal moduli) was analyzed for two values of effective nominal stress $\bar{S}$. Figure 6 shows the results for $\bar{S}$ = 100 MN/m^2. For this relatively low value of $\bar{S}$, all local stresses in the material F are in the elastic range; the corresponding local stresses in the material G extend into the plastic range. The results based on the Neuber equation correlate well with the finite-element results. The stresses from the finite-element method lie slightly off the stress-strain curves because of small errors inherent in the numerical analysis. A good correlation was also obtained for this laminate at $\bar{S}$ = 200 MN/m^2, as shown in figure 7. For this relatively high stress, maximum and minimum local stresses in both materials F and G are in the plastic range. Equation (8) was used for the Neuber curve in this case because of net-section yielding in the weaker material, G.

Figure 8 shows the results for the second laminate, composed of materials F and H (different moduli), for $\bar{S}$ = 400 MN/m^2. The results from the present method correlate well with those computed by the finite-element analysis.

The results for the third laminate, composed of Ti-6Al-4V alloy with interface layers of commercially pure titanium, are presented in figure 9 for $\bar{S}$ = 400 MN/m^2. The nine-layer laminate was represented by an equivalent two-layer laminate. The thickness of each layer in the two-layer laminate was equal to the total thickness of the material in the nine-layer laminate that it represented. The parts of the stress-strain curves corresponding to unloading from tension and subsequent compressive loading were not available from the literature. These parts of the stress-strain curves, therefore, were constructed by a procedure similar to that used for cyclic stress-strain curves in reference 15. That is, values of stresses and strains from the monotonic tensile curves were doubled and plotted from the points of maximum stress and strain to approximate the curves for unloading and compressive loading. The maximum and minimum local stresses determined for both the Ti-6Al-4V alloy and the pure titanium are in the plastic range. Again, good correlation exists between the results from the Neuber method and those from the finite-element analysis.

The results obtained for the laminates analyzed in this study are summarized in table 1. For all cases, local stresses and strains determined by the method based on the Neuber equation were very near those computed by the finite-element analysis. The estimates obtained by the method are, therefore, good approximations of local elasto-plastic stresses and strains in laminates during one loading cycle. The application of this method to determine local cyclic stresses and strains during fatigue loading may provide a rational basis for estimating fatigue life of metallurgically bonded notched laminates.

CONCLUDING REMARKS

A simple, semianalytical method was developed to determine elastoplastic cyclic stresses and strains at stress concentrations in metallurgically bonded metal laminates. It was based on the Neuber equation and an effective stress-strain curve for the laminate.

The method was applied to laminated sheets with a circular hole which were subjected to one reversed-loading cycle. The laminated materials had different combinations of yield strengths and Young's moduli. The results agreed well with those computed by a finite-element analysis. Thus, the method based on the Neuber equation yielded good approximations of local elastoplastic stresses and strains in the laminates during a loading cycle.

Langley Research Center,
National Aeronautics and Space Administration,
Hampton, Va., August 26, 1974.

REFERENCES

1. Cox, D.; and Tetelman, A. S.: Improved Fracture Toughness of Ti-6Al-4V Through Controlled Diffusion Bonding. AFML-TR-71-264, U.S. Air Force, Feb. 1[illegible].

2. Cox, D. O.; and Tetelman, A. S.: Fracture Toughness and Fatigue Properti[illegible] of Titanium Laminate Composites Produced by Controlled Diffusion Bonding. AFML-TR-73-288, U.S. Air Force, Oct. 1973.

3. Sova, J. A.; and Williams, T. R. G.: Fatigue Properties of the Alclad Al-Cu-Mg-Si-Mn Alloy. Aeronaut. J. Roy. Aeronaut. Soc., vol. 78, no. 764, Aug. 1974, pp. 375-379.

4. Staley, J. T.; and Evancho, J. W.: Development of a Cladding Alloy for 7050-T76 Sheet and Quenching Characteristics of Aluminum Alloy 7050. Contract N00019-72-C-0146, Aluminum Co. of America, Nov. 7, 1972.

5. Schijve, J.; and Jacobs, F. A.: Fatigue Tests on Unnotched and Notched Specimens of 2024-T3 Alclad, 2024-T8 Alclad and 7178-T6 Extruded Material. NLR TR 68017 U, Nat. Aerosp. Lab. (Amsterdam), Feb. 1968.

6. Neuber, H.: Theory of Stress Concentration for Shear-Strained Prismatical Bodies With Arbitrary Nonlinear Stress-Strain Law. Trans. ASME, Ser. E: J. Appl. Mech., vol. 28, no. 4, Dec. 1961, pp. 544-550.

7. Crews, John H., Jr.: Elastoplastic Stress-Strain Behavior at Notch Roots in Sheet Specimens Under Constant-Amplitude Loading. NASA TN D-5253, 1969.

8. Crews, John H., Jr.: Effects of Loading Sequence for Notched Specimens Under High-Low Two-Step Fatigue Loading. NASA TN D-6558, 1971.

9. Isakson, G.; Armen, H., Jr.; and Pifko, A.: Discrete-Element Methods for the Plastic Analysis of Structures. NASA CR-803, 1967.

10. Armen, H., Jr.; Pifko, A.; and Levine, H. S.: Finite Element Analysis of Structures in the Plastic Range. NASA CR-1649, 1971.

11. Crews, John H., Jr.: An Elastoplastic Analysis of a Uniaxially Loaded Sheet With an Interference-Fit Bolt. NASA TN D-7748, 1974.

12. Howland, R. C. J.: On the Stresses in the Neighbourhood of a Circular Hole in a Strip Under Tension. Phil. Trans. Roy. Soc. (London), ser. A, vol. 229, no. 671, Jan. 6, 1930, pp. 49-86.

13. Wood, R. A.; and Favor, R. J.: Titanium Alloys Handbook. MCIC-HB-02 (Contracts F33615-72-C-1227 and DSA900-73-C-0922), Battelle Columbus Lab., Dec. 1972. (Available from DDC as AD 758 335.)

14. Hayward, D. C.: Mechanical Properties of Ti 75A Sheet Titanium at Room and Elevated Temperatures. Tech. Note No. Met. 210, Brit. R.A.E., Nov. 1955.

15. Morrow, JoDean: Cyclic Plastic Strain Energy and Fatigue of Metals. Internal Friction, Damping, and Cyclic Plasticity, Spec. Tech. Publ. No. 378, Amer. Soc. Testing Mater., 1965, pp. 45-87.

TABLE 1.- LOCAL STRESSES AND STRAINS FOR ONE CYCLE OF REVERSED LOADING

Laminate	Materials	$\bar{S}$, MN/m^2	E, MN/m^2	Yield strength, MN/m^2	Local stress, σ, MN/m^2, and local strain, ϵ, percent															
					Maximum				Half-cycle residual				Minimum				Full-cycle residual			
					Neuber		Finite element		Neuber		Finite element		Neuber		Finite element		Neuber		Finite element	
					σ	ϵ	σ	ϵ	σ	ϵ	σ	ϵ	σ	ϵ	σ	ϵ	σ	ϵ	σ	ϵ
1	F	100	68 950	500	327	0.473	323	0.470	42	0.060	49	0.071	-327	-0.473	-323	-0.470	-42	-0.060	-49	-0.071
	G			100	100		105		-100		-104		-100		-105		100		104	
	F	200	68 950	500	500	2.021	505	1.950	-155	1.070	-164	0.098	-500	-2.021	-505	-1.950	155	-1.070	164	-0.098
	G			100	100		103		-100		-108		-100		-103		100		108	
2	F	400	68 950	500	500	1.078	505	1.010	-30	0.310	-23	0.[illegible]2	-500	-1.078	-505	-1.010	30	-0.310	23	-0.242
	H		206 950	1000	1000		1010		-583		-574		-1000		-1010		583		574	
3	Ti-6Al-4V	400	110 320	827	923	1.175	930	1.150	-380	0.207	-381	0.175	-923	-1.175	-930	-1.150	380	-0.207	381	-0.175
	Ti			380	550		555		-141		-148		-550		-555		141		148	

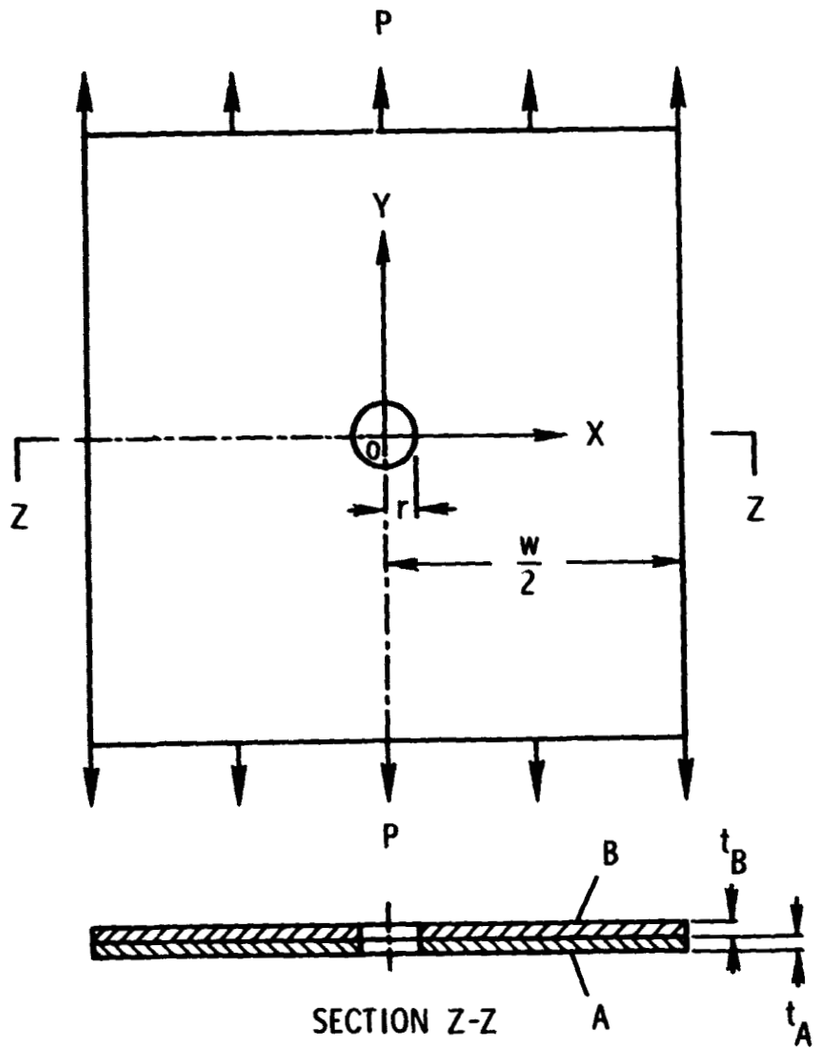

Figure 1.- Notched laminate subjected to uniaxial load.

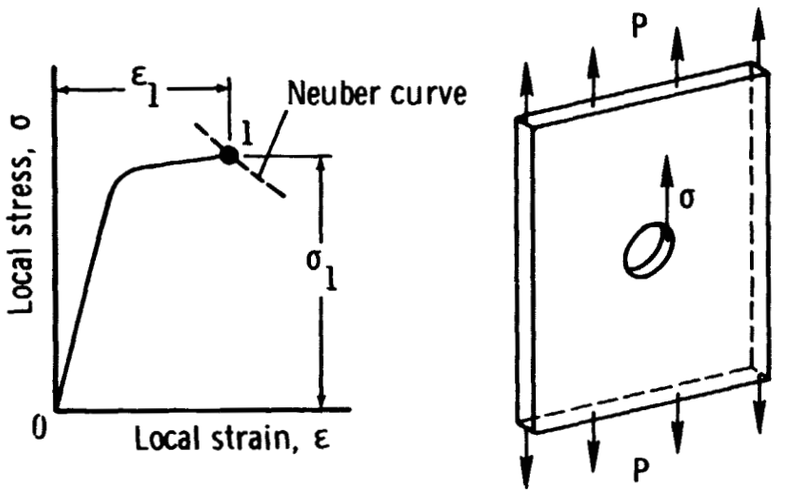

(a) Single sheet.

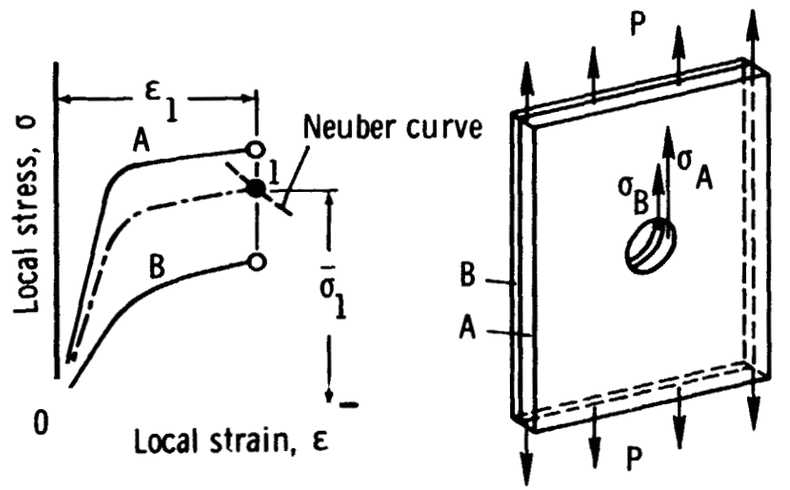

(b) Laminate.

Figure 2.- Local stress-strain curves for monotonic loading.

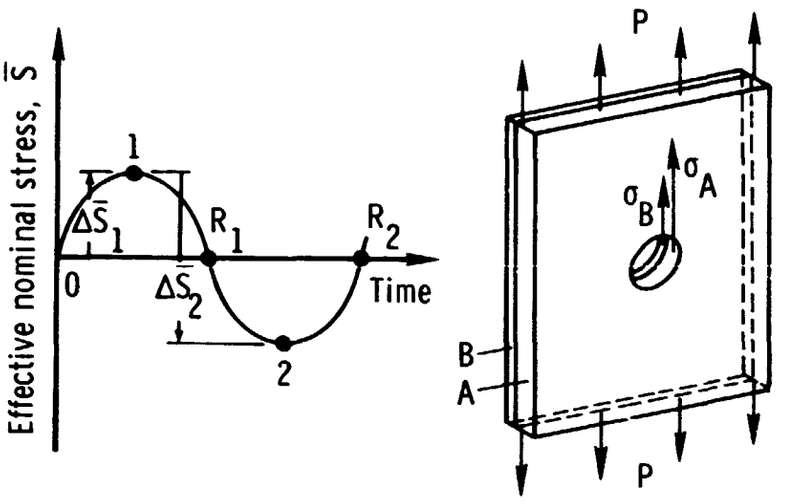

(a) Effective nominal stress cycle.

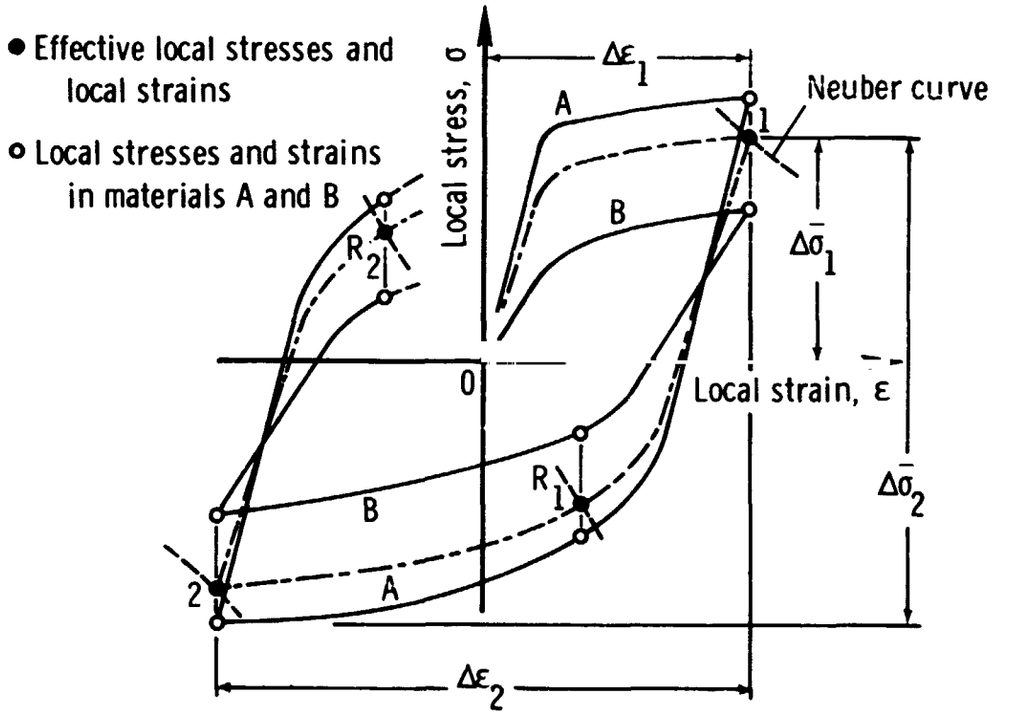

(b) Local stress-strain curves.

Figure 3.- Local stress-strain curves for cyclically loaded laminate.

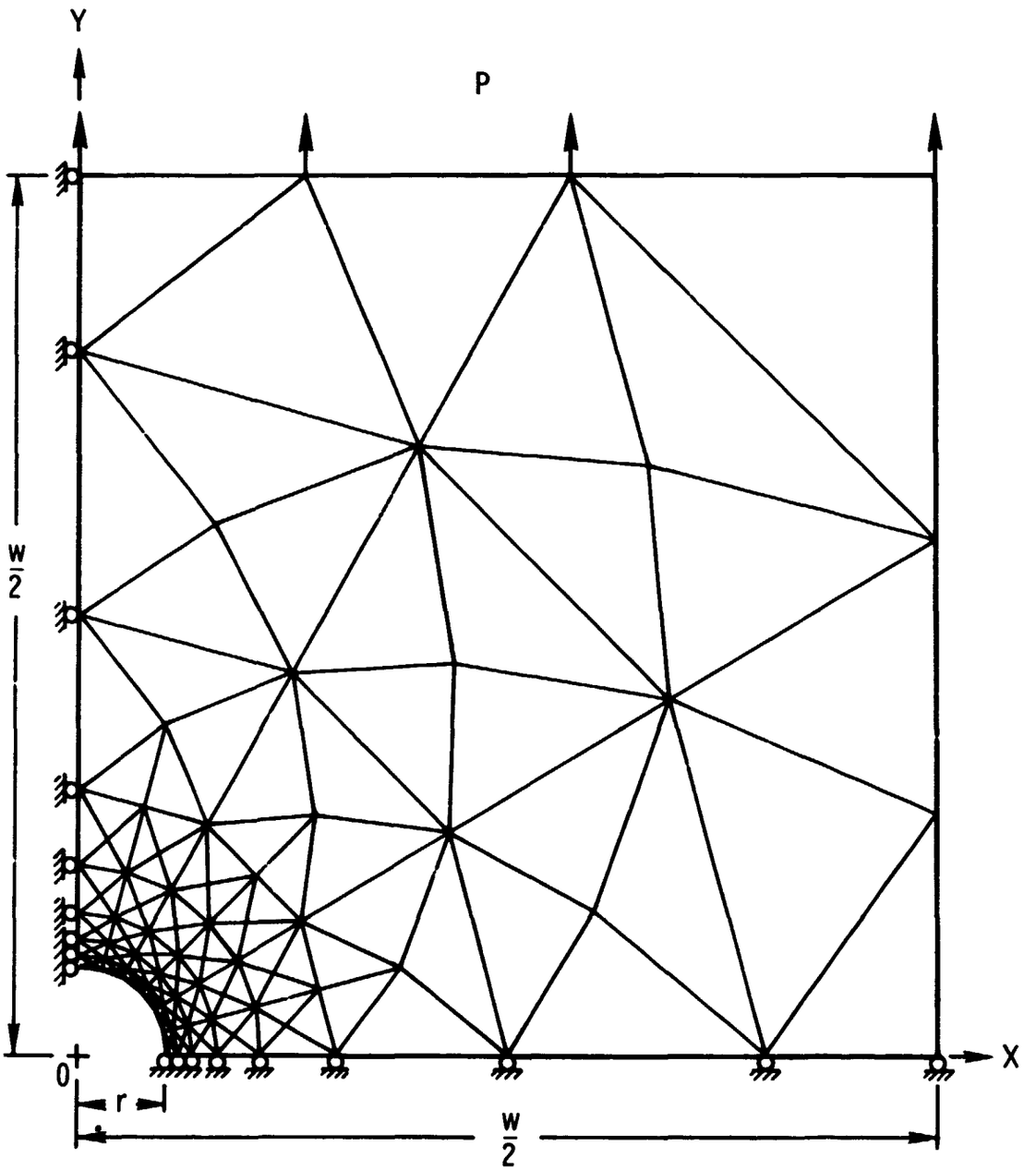

Figure 4.- Finite-element model for notched laminate.

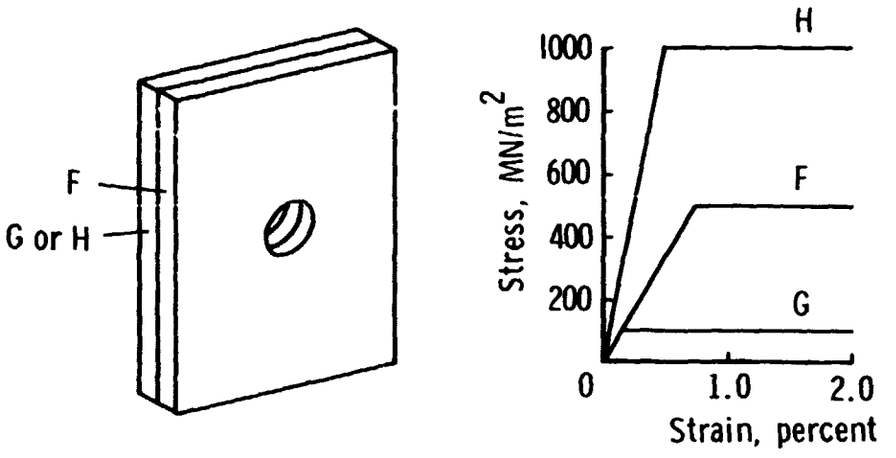

(a) Elasto-perfectly-plastic laminates.

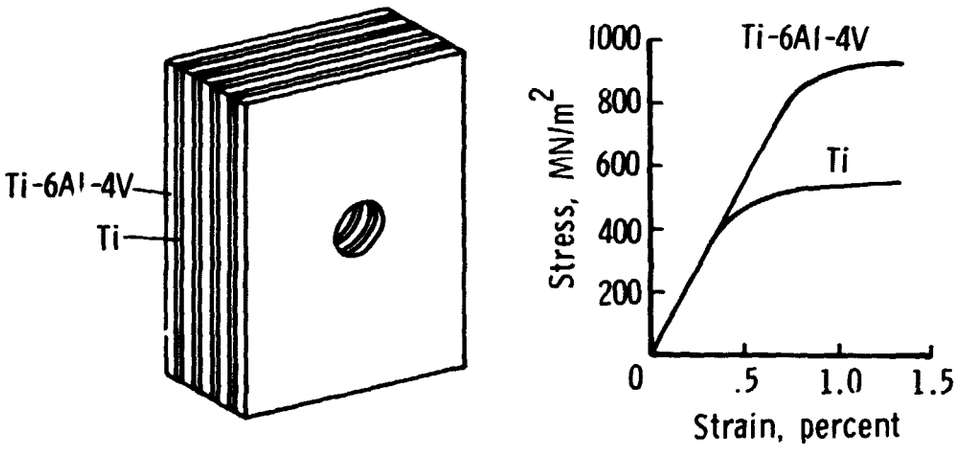

(b) Laminate of Ti and Ti-6Al-4V.

Figure 5.- Selected laminates and stress-strain curves for individual materials.

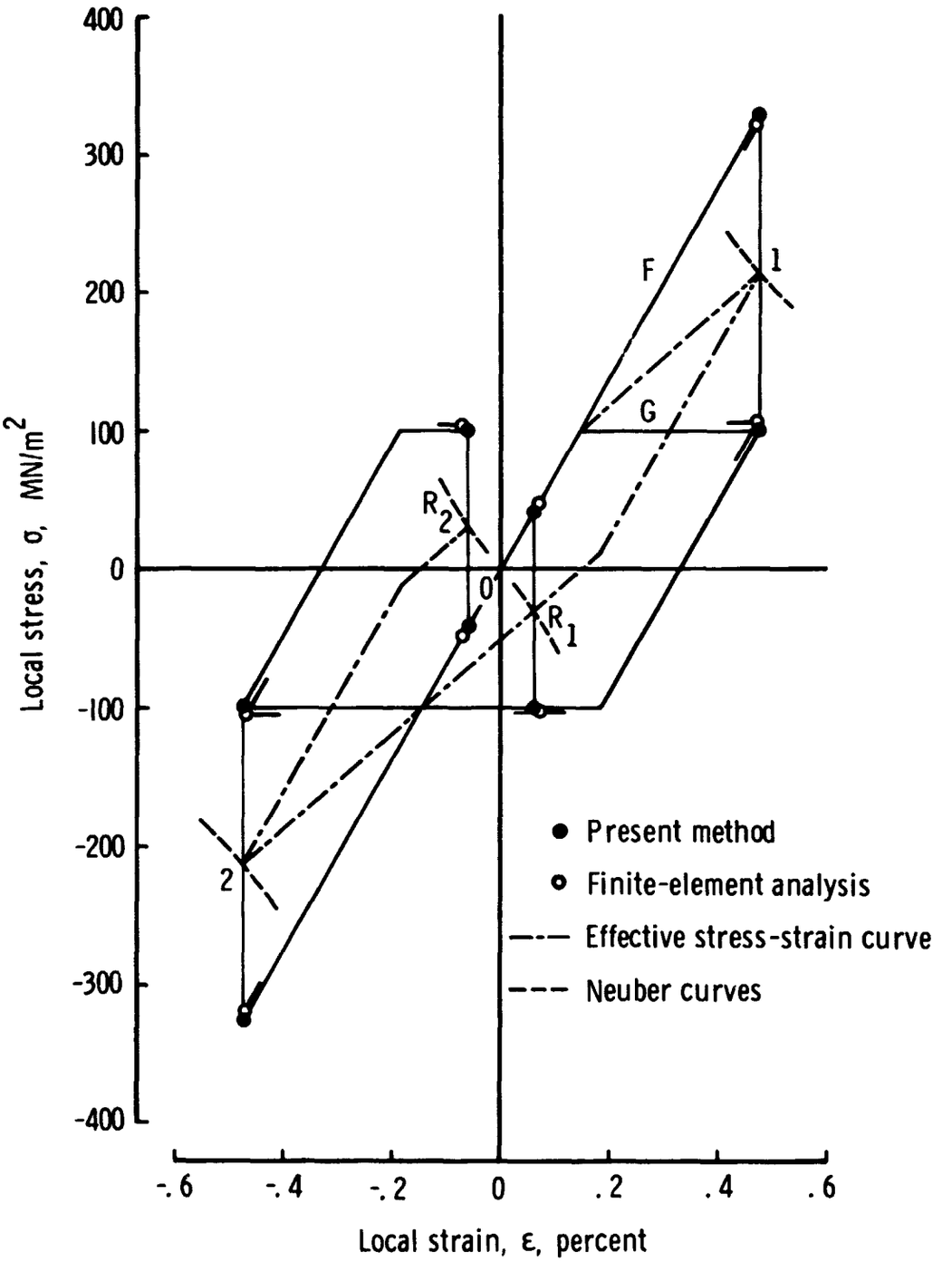

Figure 6.- Local stress-strain curves for laminate of materials with different yield strengths and equal moduli. $\bar{S}$ = 100 MN/m^2.

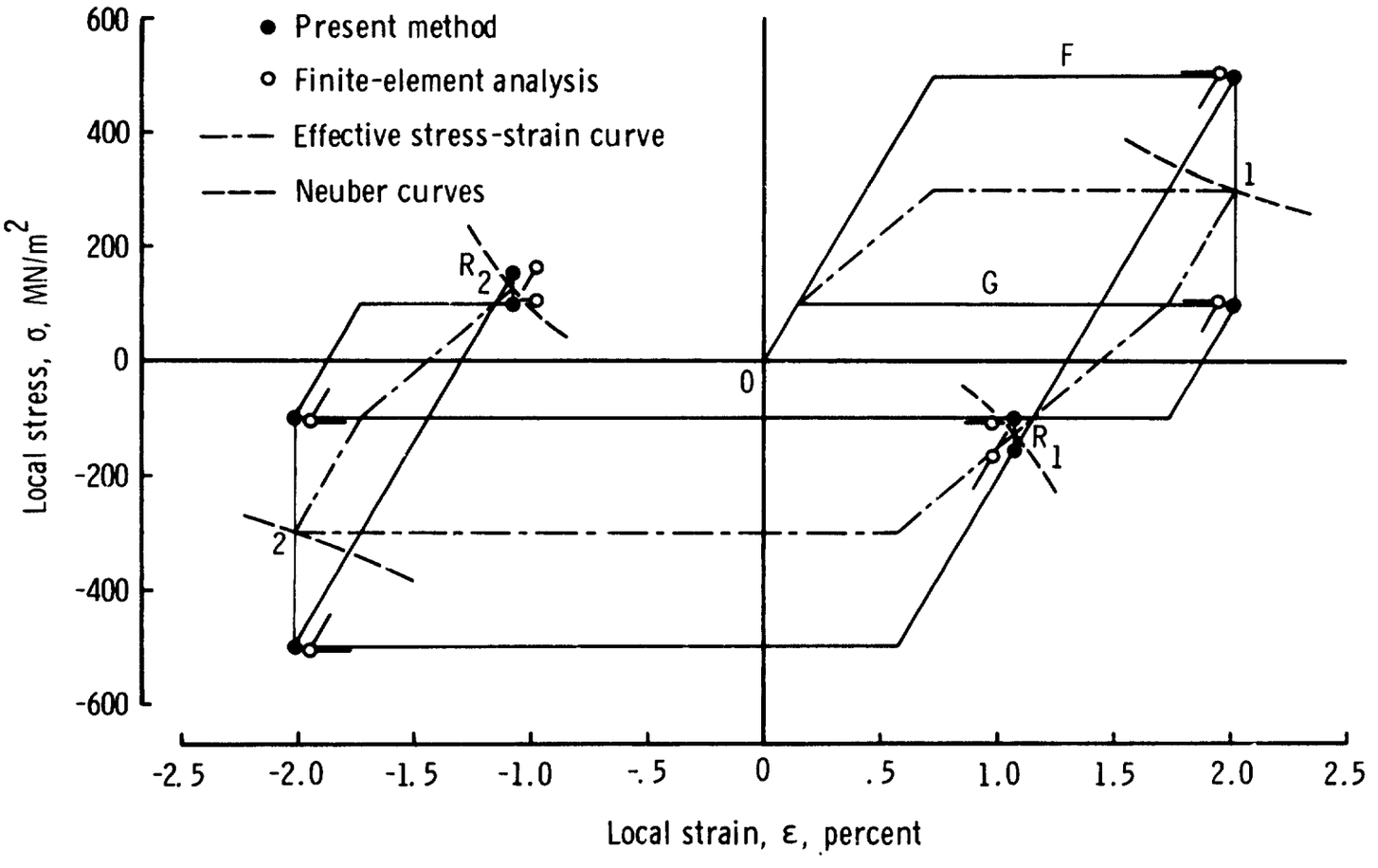

Figure 7.- Local stress-strain curves for laminate of materials with different yield strengths and equal moduli. $\bar{S}$ = 200 MN/m^2.

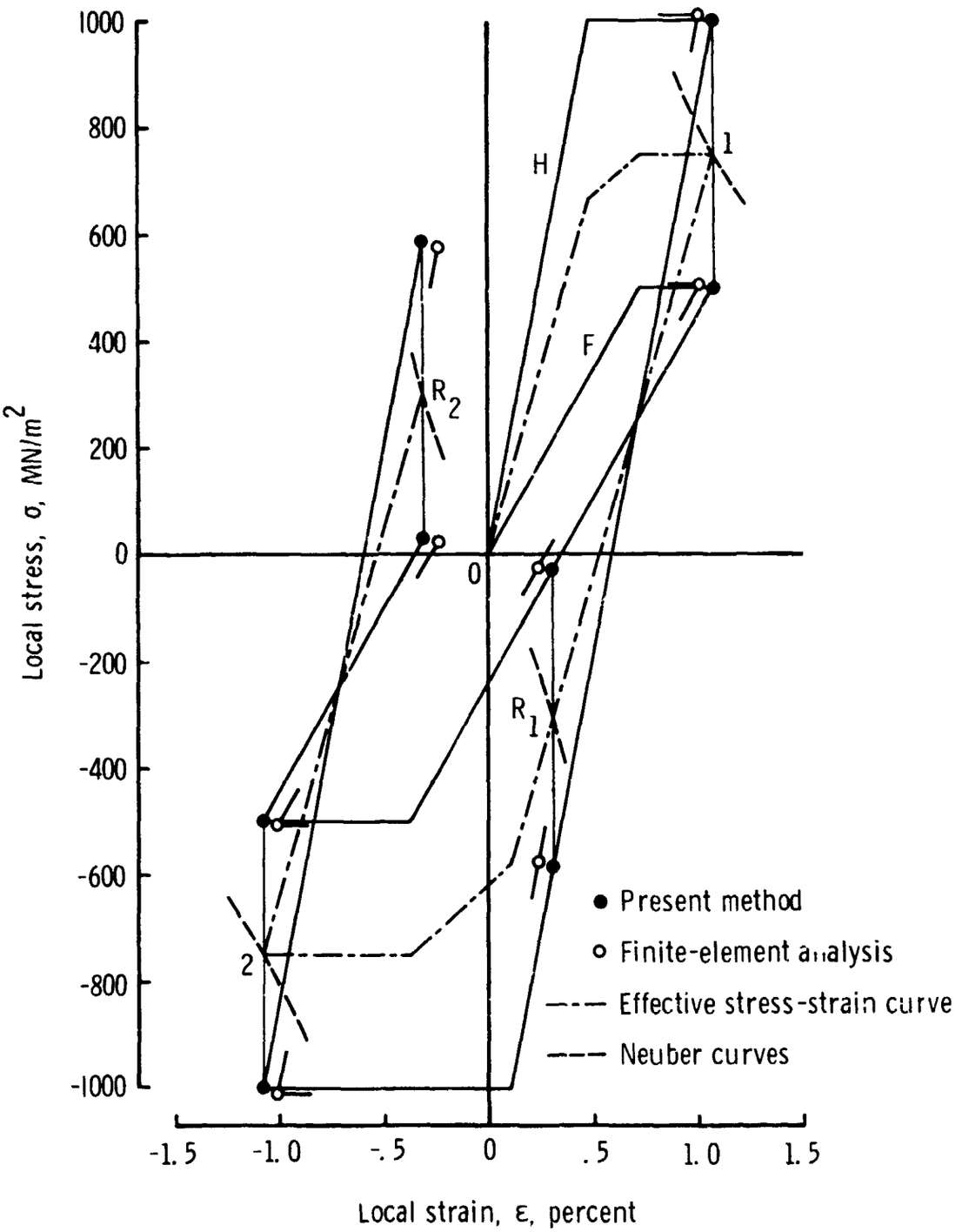

Figure 8.- Local stress-strain curves for laminate of materials with different yield strengths and moduli. $\bar{S}$ = 400 MN/m^2.

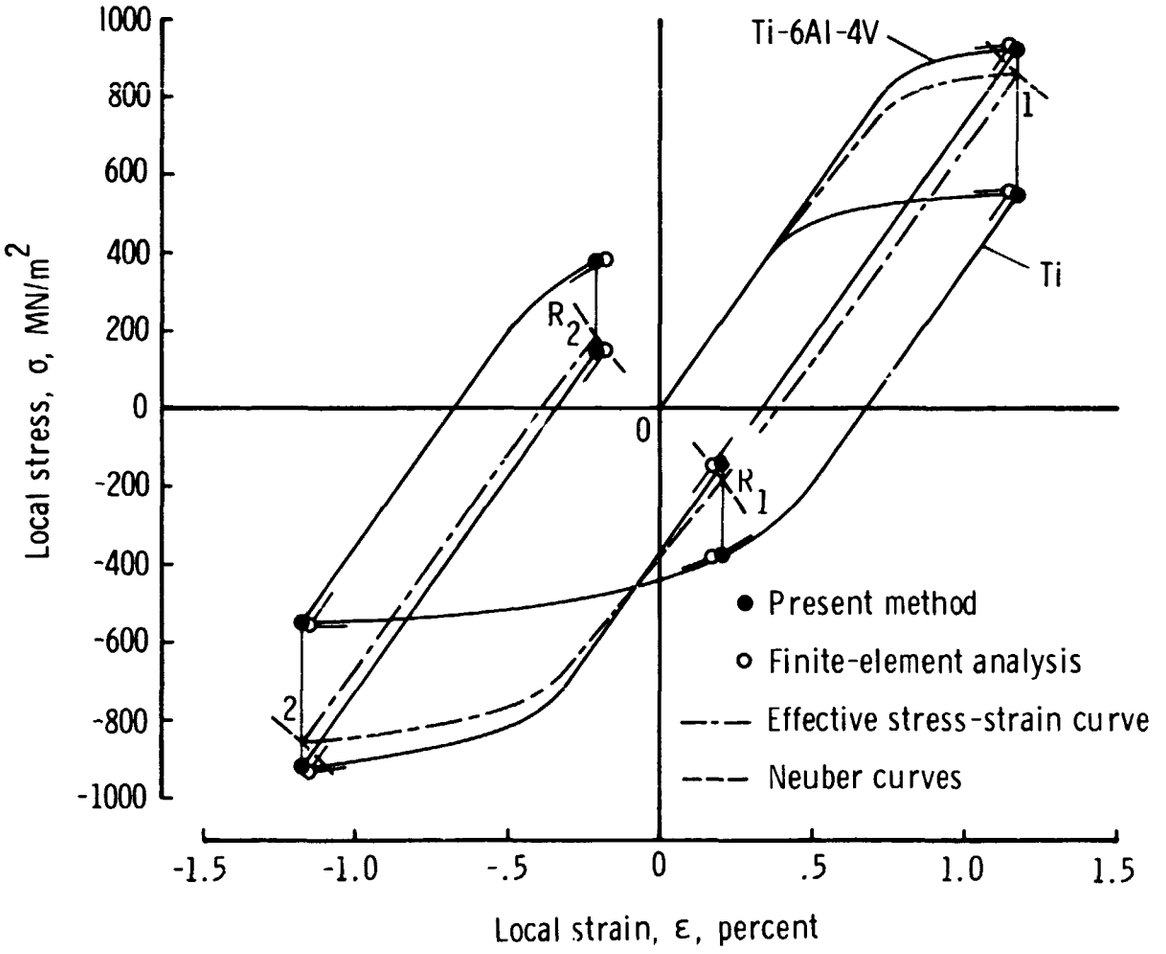

Figure 9.- Local stress-strain curves for laminate of Ti-6Al-4V and Ti. $\bar{S}$ = 400 MN/m^2.